Science of the Total Environment 760 (2021) 143898

Contents lists available at ScienceDirect

Science of the Total Environment

journal homepage: www.elsevier.com/locate/scitotenv

Microplastics in the Black Sea sediments

Alessandra Cincinelli [a,b,c,*], Costanza Scopetani [a], David Chelazzi [a,b], Tania Martellini [a,b], Maria Pogojeva [d,e], Jaroslav Slobodnik [f]

[a] Department of Chemistry "Ugo Schiff", University of Florence, 50019, Sesto Fiorentino, Florence, Italy
[b] Consorzio Interuniversitario per lo Sviluppo dei Sistemi a Grande Interfase (CSGI), 50019, Sesto Fiorentino, Florence, Italy
[c] National Interuniversity Consortium for Environmental Sciences (CINSA), Florence/Venice, Italy
[d] N.N.Zubov's State Oceanographic Institute, Roshydromet, 6, Kropotkinskii Lane, 119034 Moscow, Russia
[e] Shirshov Institute of Oceanology, Russian Academy of Sciences, 36, Nahimovskiy prospekt., 117997, Moscow, Russia
[f] Environmental Institute, Okruzna 784/42, 97241 Kos, Slovak Republic

HIGHLIGHTS

- First evaluation of microplastics in the sediment samples from the Black Sea.
- Results showed the evidence of microplastics in the Black Sea sediment samples.
- FTIR analysis showed the predominance of polyethylene/polypropylene, polyamides, and acrylate copolymers.

GRAPHICAL ABSTRACT

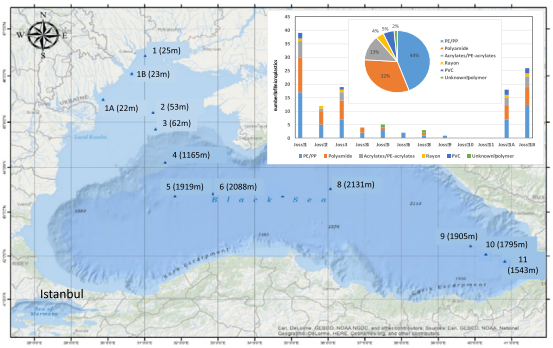

ARTICLE INFO

Article history:
Received 24 August 2020
Received in revised form 17 November 2020
Accepted 17 November 2020
Available online 2 December 2020

Editor: Damia Barcelo

Keywords:
Microplastic
Sediment
Black Sea
FT-IR
Marine pollution

ABSTRACT

In this study the occurrence, morphology and identification of microplastics in Black Sea sediments collected at different depths (range 22–2131 m) were determined for the first time. The study explored the advantages and limitations of using a non-invasive method consisting of filtration of the supernatant from the mixture of sediment with saturated NaCl solution followed by FTIR 2D imaging for the identification of natural and synthetic polymers. The proposed method confirmed its potential for clear identification of polyethylene, polypropylene, acrylonitrile, polyamides and cellulose-based fibers, but more difficulties when the filter substrate neighboring the fibers exhibits intense absorptions in the 1800–1000 cm^{-1} range.
Microplastics (MPs) were determined in 83% of the investigated sediment samples. The average abundance in all samples was 106.7 items/kg. The highest pollution occurred on the North-Western shelf where the abundance of MPs was 10 times higher than in sediments from the deep sea. The most abundant plastic polymers were polyethylene and polypropylene, followed by acrylate and acrylonitrile copolymers. Polyamide and cellulose-based textile fibers were also found. The most frequent microplastic colors observed were black, blue and clear/transparent, while fibers represented the dominant microplastics in sediments.

1. Introduction

The Black Sea is one of the most degraded ecosystems (BSC, 2007) in the world given its limited exchange of water with the open oceans and the intensive loads of pollutants carried on by large

* Corresponding author at: Department of Chemistry "Ugo Schiff", University of Florence, 50019, Sesto Fiorentino, Florence, Italy.
E-mail address: acincinelli@unifi.it (A. Cincinelli).

https://doi.org/10.1016/j.scitotenv.2020.143898
0048-9697/

European rivers run off, such as Danube, Dniester, Don, Southern Bug, Dnieper and Kubani.

According to an environmental survey funded by the European Union and the United Nations Development Programme (UNDP), the Black Sea has twice as much floating macro litter, dominated by plastic, as Mediterranean (Slobodnik et al., 2017). In particular, Lechner et al. (2014) presented results from a two-year (2010 and 2012) survey on plastic litter in the Danube (the second largest river in Europe) and estimated that 4.2 t of plastic reached the Black Sea via the river per day. In general, only 10% of plastic litter comes from fishing and shipping activities, whereas the remaining 90% is from land sources, such as rivers run-off, coastal cities, ports, wastewater treatment plants, uncontrolled coastal landfills (Andrady, 2011). However, the Black Sea is one of the major fishing areas in the world (FAO, 2015), thus this activity could also contribute with a high load of plastics to the marine environment. In the last decade, plastic litter has gained increasing attention from researchers, stakeholders, regulatory authorities, and public, both locally and globally, for its impacts in oceans and freshwaters around the world. In particular, microplastics (MPs), defined as plastic particles with a diameter less than 5 mm, may originate from the breakdown of larger plastic litter through i.e. degradation by UV-radiation, physical forces, or be already manufactured in such small size (i.e. use in cosmetic products). MPs have been found in aquatic environments, including beaches, in ocean surface waters, deep sea sediments, freshwater lakes and tributaries (Ballent et al., 2016; Andrades et al., 2018; Scopetani et al., 2019), and there are growing concerns about their potential hazard effects on biota, because its size allows its interactions with marine organisms (Cole et al., 2011). Moreover, MPs and their associated or adsorbed toxic chemicals might lead to more negative effects on ecosystems and human health. MPs can float at the sea surface or sink and accumulate in the sediments.

A recent study (Aytan et al., 2016) determined MPs from zooplankton samples collected during two cruises along the Southeastern coast of the Black Sea between 2014 and 2015 and found a prevalence of fibers (49.4%), followed by films (30.6%) and fragments (20%), and average concentrations of $1.2 \pm 1.1 \times 10^3$ p m^{-3} in November 2014 and $0.6 \pm 0.55 \times 10^3$ p m^{-3} in February 2015, respectively.

In the present contribution, MPs identification was performed using a Focal Plane Array (FPA) FTIR 2D Imaging without any potentially invasive pre-treatment of the samples. In fact, FPA detector, with enhanced spatial resolution (from ca. 1 to 5 μm), has emerged as an advantageous method to identify MPs, as it allows to identify small MPs on relatively large areas (millimeters or centimeters) in short times (Harrison et al., 2012; Löder et al., 2015; Tagg et al., 2015). Moreover, a recent paper has shown the detection and identification of MPs using FPA detectors even on complex biogenic matrices (Cincinelli et al., 2017), without the need to separate the plastic samples from the filters and membranes where they are collected, so to avoid lengthy processes or alteration of the samples.

Until now, only a limited number of global surveys have been conducted on the quantity and distribution of microplastics in the oceans (Lusher, 2015). Especially, there is only limited information on MPs in deep sediments and no data is available for sediments in the Black Sea. Under the EU/UNDP project "Improving Environmental Monitoring in the Black Sea (EMBLAS-II)", in cooperation with the governments and research institutions of Georgia, Russian Federation and Ukraine, different research activities were conducted in 2016 and 2017 (Slobodnik et al., 2017) to achieve critical amount of data needed to assess indicative environmental status of the Black Sea, in line with the Marine Strategy Framework Directive (MSFD) and the Black Sea Strategic Action Plan needs. According to the knowledge of the authors, in the present

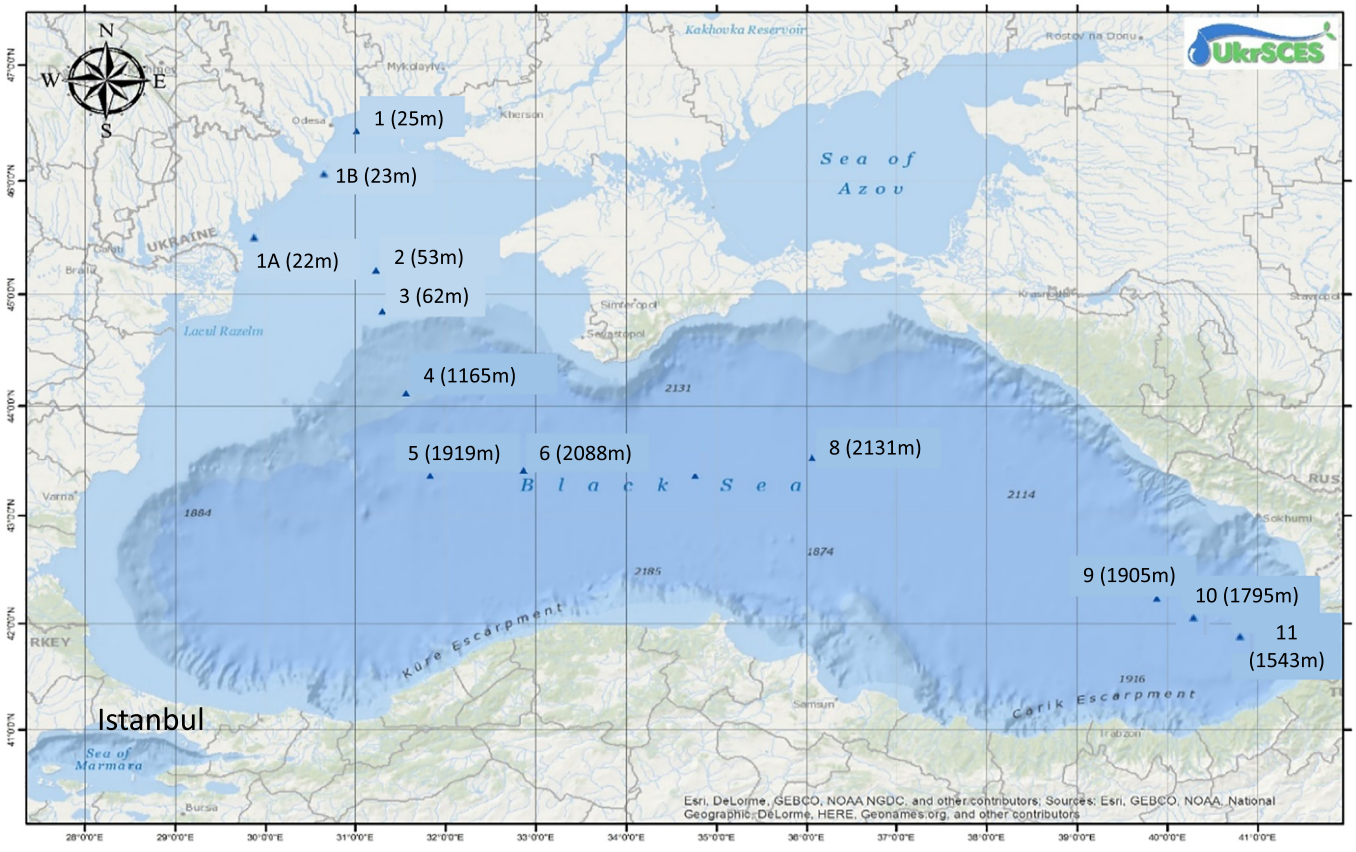

Fig. 1. An overview map of the sampling stations during the Joint Open Sea Survey 2017 (for a list see Table S1) and water depth for each sampling station.

study the occurrence, morphology and identification of MPs in Black Sea sediments collected at different depths (range 22–2131 m) were determined for the first time.

2. Materials and methods

2.1. Sample collection

Undisturbed sediment samples were collected, under calm conditions, on two latitudinal transects across the Black Sea, using Van Veen grab and Box corer sampling techniques in order to reach different depths, ranging 22–62 m and 1165–2131 m, respectively. Sample names, locations, coordinates and water depths were detailed in Supplementary Information (Table S1). A total of 12 sediment samples (about 5 cm depth) was collected (see Fig. 1, with relative water depth for each sampling station) and frozen at −20 °C until analysis.

2.2. Microplastic extraction

All sample extractions were performed in a clean room and under a laminar flow hood, in order to avoid any potential contamination (Scopetani et al., 2020). In addition, the laboratory surface was routinely wiped down and all beakers, containers, funnels and tools were washed, rinsed with filtered deionized water (0.8 μm membrane filter) before and after each use, and stored covered in aluminum foil. As additional precautions, all clothes in the lab were made of cotton and/or natural fibers and the materials used for analysis were made of glass or stainless steel when possible. Potential airborne microplastic contamination during sample processing was determined by exposing damp filter paper to the air in the laboratory.

All samples were treated according to the procedure described in detail below, which refers to "DeFishGear Protocols for sea surface and beach sediment sampling and sample analysis", with some modifications. Briefly, 100 g of dry sediments were analyzed for each sample. Aliquots of 25 g were put in a glass beaker and then a saturated NaCl solution was added and shaken for 2 min and left for sedimentation. After 2 h, the solution was decanted. The supernatant, which contained the plastic items, was filtered through a Büchner glass funnel. The extraction was repeated three times for each sample, using the same glass filter (pore size 0.49 μm) to increase recovery efficiency. The use of NaCl saturated solutions is recommended since it is an unexpensive and eco-friendly salt (Galgani et al., 2013).

The use of a NaCl saturated solution for microplastic extraction showed for spiked artificial sand samples with MPs (PE, PP, PS, and PU) a mean MPs spiked recovery rate of 85 ± 3%, while for PVC and PET the mean recovery was 67 ± 3%. These data are in good agreement with what is reported by Quinn et al. (2017). The collected fibers were classified according to size, shape and color categories.

2.3. 2D imaging-Fourier transform infrared

The 2D imaging-Fourier transform infrared (FTIR) analysis of the microfibers was carried out directly on the dry filters (with no further sample preparation) using a Cary 620–670 FTIR microscope, equipped with an FPA 128 × 128 detector (Agilent Technologies). The spectra were recorded directly on the surface of the samples (or of the Au background) in reflectance mode, with open aperture and a spectral resolution of 8 cm^{-1}, acquiring 128 scans for each spectrum. A "single-tile" analysis results in a map of 700 × 700 μm^2 (128 × 128 pixels), and the spatial resolution of each Imaging map is 5.5 μm (i.e. each pixel has dimensions of 5.5 × 5.5 μm^2). All fibers were analyzed with this method. In each 2D map, the intensity of characteristic bands of the investigated polymer was imaged. The chromatic scale of the maps shows increasing absorbance of the bands as follows: blue < green < yellow < red.

3. Results and discussion

3.1. Microplastic abundance and polymer composition

A total of 128 items were identified as microplastics. 12 samples of bottom sediments were analyzed. MPs were found in 10 out of 12 samples (83%). MPs were not found in the sediment samples from the sites JOSS-GE-UA-10 and JOSS-GE-UA-11, however it does not imply that no MPs were present there at all as at each site only one sample was taken with too small volume of sediments (about 100 g). The abundances varied between 0 and 390 items/kg, and the average number is 106.7 items/kg.

Five out of twelve samples were taken in the depths less than 62 m, the average abundance of MPs there was 226 items/kg. Other 7 samples from the depths more than 1000 m, showed an average abundance 21.4 items/kg. So, the abundance of MPs on the shelf was much higher than in the deeper open sea sediments (Fig. 2).

Maximum microplastics abundance was found at site JOSS-GE-UA-1 (390 items/kg), a nearshore sediment, followed by JOSS-GE-UA-1B (260 items/kg) and JOSS-GE-UA-3 (180 items/kg) sediments. All these stations are situated in the North-Western shelf, a discharge area for major rivers, such as the Danube and Dnieper, flowing into the Black Sea. Their large drainage area, a lot of industrialized cities on their banks as well as constantly increasing density of population along the coast lines lead to elevated levels of pollution in their waters. River run-off is among the main sources of the Black Sea pollution and the highest contribution is expected from the Danube River comprising ca. 80% of the total river flow input (Slobodnik et al., 2017). A recent study estimated that 4.2 t of plastic reach the Black Sea via the Danube per day (1533 t every year) (Lechner et al., 2014). Long-term investigations also show that main ecological problems of the Black Sea are most actually showing in the inshore and in the shelf zones, where the maximal influence of the sources of contamination is being observed (State of the Black Sea Environment, 2002).

Comparing the spatial distribution of MPs with the floating litter data received during the Joint Black Sea Survey 2017 (Fig. 4), we can see that the high density transects on the North-Western shelf correlate well with high abundances of MPs in sediments in the same region, however there is no correlation on the Eastern part of the route where the floating litter observations showed very high densities, but no MPs was found in these samples. This could also relate to the small size of sediment samples. For more informative conclusions further monitoring with improvements of the applied sampling methodology is needed.

Microplastic contamination loads in Black Sea sediments are comparable to those reported in other European seas, such as North Sea locations, harbours and beaches in Belgium (Claessens et al., 2011), Jade System in Germany (Dubaish and Liebezert, 2013), and in sediments from the Changjiang Estuary (China) (Peng et al., 2017) but lower

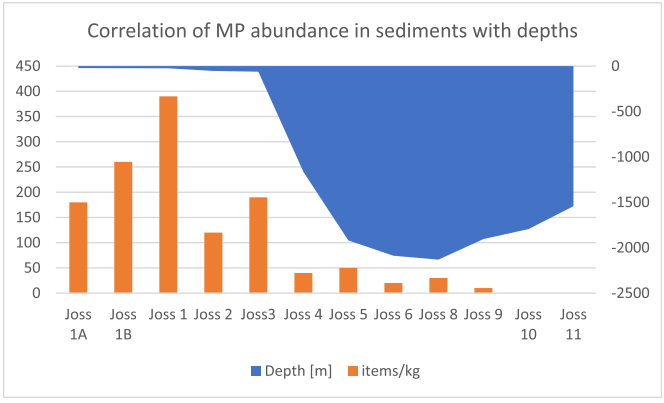

Fig. 2. The abundance of microplastics in the sediments along the JOSS profile.

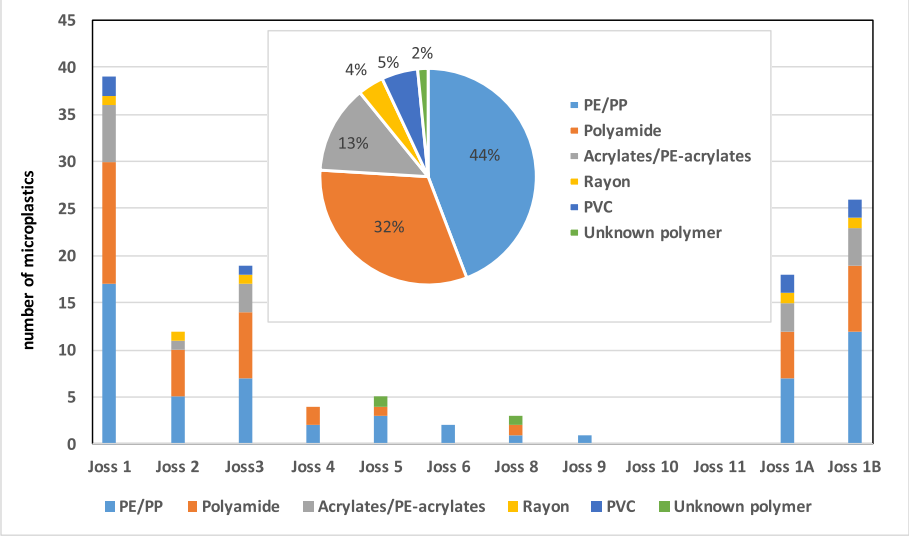

Fig. 3. Types of polymers and number of microplastics found in the sediment samples.

than those determined in Mediterranean Sea sediments, such as in Venice lagoon (Vianello et al., 2013) and in a canal in Tokio Bay (Japan) (Matsugama et al., 2017). However, MP concentration in marine sediments from around the world may also vary significantly because different factors may play a fundamental role for abundance of plastic pollution. Moreover, the lack of a standardized sampling protocol, which leads to different units (items m^{-2}, items kg^{-1}) of microplastic abundance, makes the comparability of data more difficult.

The most frequent microplastic colors observed were black, blue and clear/transparent.

As also evidenced by Claessens et al. (2011), fibers were dominant in sediments. Fibers varied in color (47.7% black, 28.1% blue, 4.7% light blue, 7% red, 3.1% violet, 3.9% green and 5.5% transparent) and lengths, from tens of microns (most abundant in near shore samples) to several millimeters.

Various polymer types were found, including polyethylene and polypropylene (PE/PP), polyamide, acrylate and acrylonitrile and cellulose (see Fig. 3). The relative abundance of each type of MP was as follows: PE/PP (44.5%), polyamide (32.0%), acrylates and polyethylene-acrylate copolymers (13.3%), cellulose (3.9%), PVC (4.7%) and not-identified polymers (1.6%).

The sea floor can be considered a sink for marine plastic but the deposition mechanisms are still not clear (Goldberg, 1997). In general, dense plastics such as nylon (about 1.12–1.15 g cm^{-3}), PVC (1.38–1.41 g cm^{-3}) and polyethylene terephthalate (PET) (1.38–1.41 g cm^{-3}) tend to sink in the water column and deposit in the

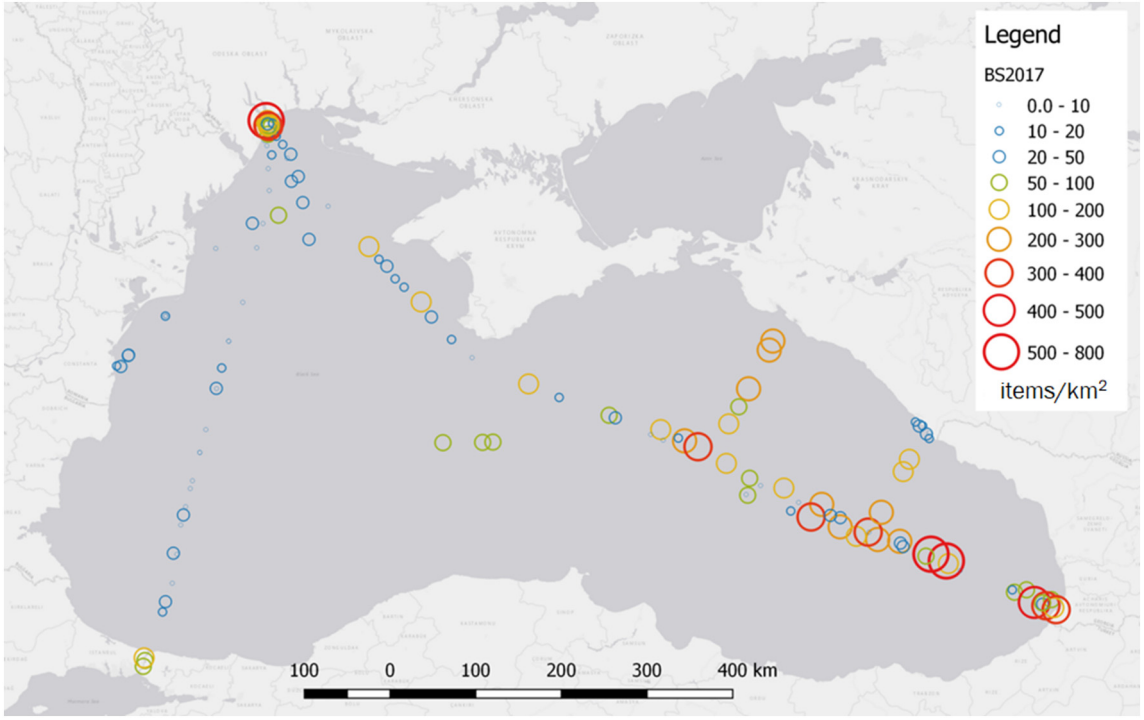

Fig. 4. Floating Marine Macro Litter – densities of the transects uploaded during the cruises in 2017 (Slobodnik et al., 2017).

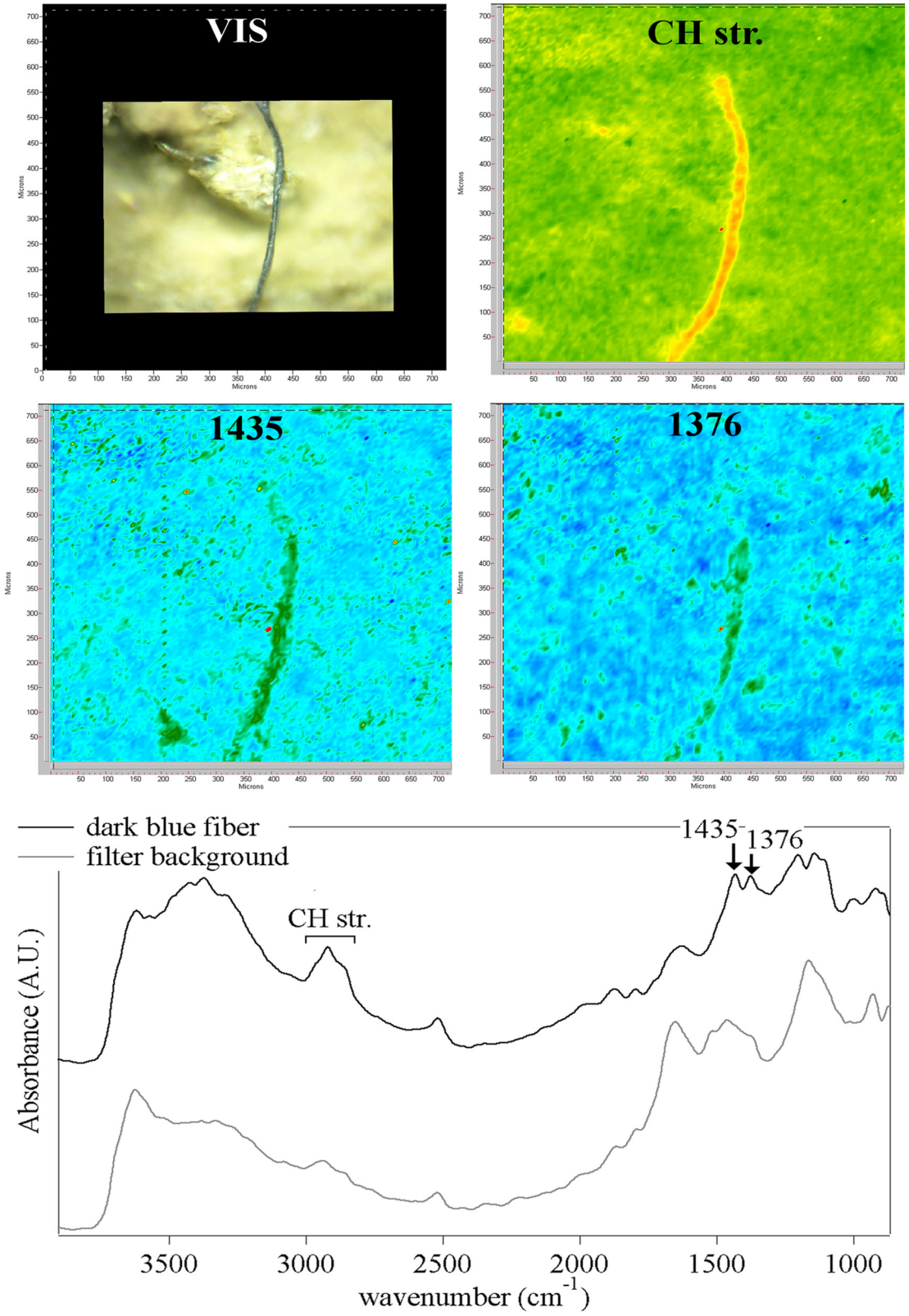

Fig. 5. Dark blue fiber - (Top left) Visible light map of the filter substrate, with marine sediments and a plastic microfiber lying on it. (Top right and center panels) 2D FTIR Imaging maps, where the intensity of the following bands was mapped: 3000–2800 (CH stretching region), 1435 (δ_{as} CH_2), and 1376 cm^{-1} (δ_s CH_3). The chromatic scale of each map qualitatively shows the absorbance intensity as follows: blue, green, yellow, red. Maps have dimensions of 700 × 700 μm^2 (1 tick = 50 μm). The bottom panel shows the FTIR Reflectance spectra of the plastic microfiber and of the filter substrate. Each spectrum relates to a single pixel (5.5 × 5.5 μm^2) of the 2D Imaging maps. (For interpretation of the references to color in this figure legend, the reader is referred to the web version of this article.)

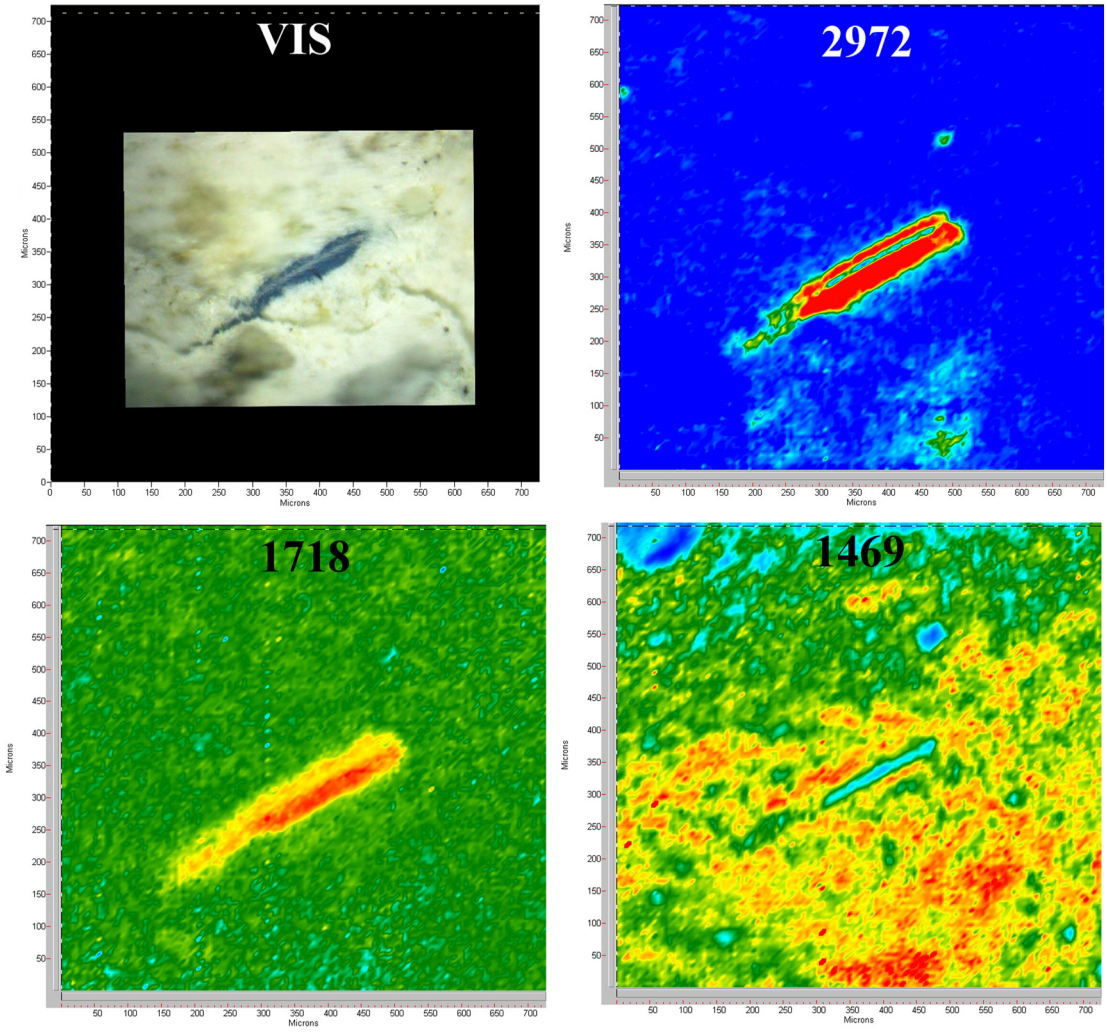
VIS
2972
1718
1469
Microns

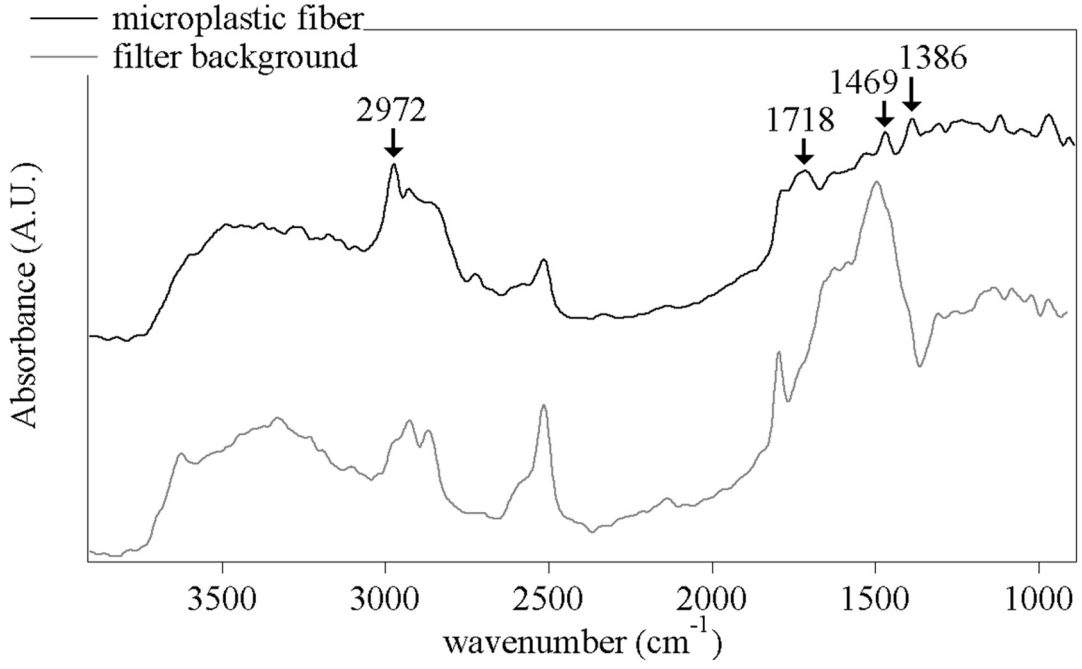
microplastic fiber
filter background
2972
1718
1469
1386
Absorbance (A.U.)
3500
3000
2500
2000
1500
1000
wavenumber (cm-1)

sea floor (Andrady, 2011), while PE (0.85–0.92 g cm^{-3}) and polystyrene (PS) (1.04–1.06 g cm^{-3}) will prefer to float at the sea surface (Vianello et al., 2013). However, the low presence of high-density MPs in our sediment samples could be due to the choice of the NaCl saturated solution used for the MPs extraction, which is able to lift preferentially MPs with similar density. The presence of less dense plastics, such as PE and PP, could be related to the possible biofouling of floating plastic items that could increase their density and favor their transport/sink to the sea floor (Lobelle and Cunliffe, 2011). This transport could be also influenced by sea water turbidity, due to storms and wind, which imply surface mixing and consequent redistribution of light MPs in the water column, and also to degradation which may change the apparent density of polymers.

The spatial distribution and abundance of microplastics were matching well observations in other seas (Kane and Clare, 2019). The results showed the predominant abundance of PE/PP, polyamide and acrylate MPs in the samples. This trend correlates well with the global plastics production according to Brien (2007), where PE (used in production of plastic bags, bottles, netting, drinking straws) amounts to 38% and PP (commonly used for ropes, bottle caps, netting) reaches 24% of plastics production in the world. Consequently, PE and PP in particular have high likelihood of ending up in the ocean environment (Andrady, 2011).

The neutral to negative buoyancy of polyamide may also lead to its accumulation at depth (Cole et al., 2016). In fact, high concentrations of polyamide fibers (i.e. nylon) were expected based on maritime usage, in particular fishing activities.

The composition of samples in Black Sea sediments included manmade and natural fibers such as acrylonitrile and cellulose-based. Acrylates could derive from synthetic textiles; thus, laundering could be a (Andrady, 2011; Aytan et al., 2016; Ballent et al., 2016) source of MPs in sewage treatment plants, whose outlets enter the marine environment.

Cellulose-based fibers were also identified prevalently in sediments from lesser depths. Cellulose fibers were included in our results as they comprise commercial textiles (e.g. cotton) and manufactured fiber made from regenerated cellulose (e.g. rayon), which are widely reported as present in the marine environment. For instance, rayon possesses a range of well-known properties, including flame retardants and super absorbent ability, meeting the demands for a wide variety of uses. Rayon is used in cigarette filters, personal hygiene products (e.g. wipes, napkins) and clothing, and it may be introduced to the marine environment through wastewater and sewage, including the input from washing machines (Frias et al., 2016). High percentage of regenerated cellulose fibers in sediments were recently published by Woodall et al. (2014), regarding deep sea sediments from NE Atlantic, Mediterranean, SW Indian, subpolar North Atlantic, and by Frias et al. (2016), reporting MPs data in coastal sediments from Southern Portuguese shelf waters. Rayon has also been documented in fish samples (57.8% of synthetic particles ingested) (Lusher et al., 2013) and in ice cores (54%) (Obbard et al., 2014).

Geographical aspects of the Black Sea like high isolation from the World Ocean, the drainage area which exceeds its surface many times, enormous recreational and maritime uses of the sea, as well as constantly increasing population along the coast line make it specifically exposed for microplastics accumulation.

3.2. Identification of MPs by 2D FTIR imaging

2D FTIR Imaging was performed to validate MP identification and facilitate comparison with other studies. The scope of the 2D Imaging FTIR analysis was to identify the fibers deposited on, or embedded in, a composite inorganic-organic substrate that included glass fiber (the filter), calcium carbonate, sand and algae coming from marine sediments. The main challenge is due to the presence of several bands in the spectra of the substrate, which interfere with those of the plastic polymers. It should be noted that the distribution of the different components (organic, inorganic) of the substrate is highly heterogeneous across the full field of view of the IR microscope (700 × 700 μm^2). Therefore, subtracting the spectra of the substrate from those of the analytes did not make the assignment of the polymers' bands significantly clearer. Nonetheless, it was possible to identify different classes of polymers by direct imaging of diagnostic bands. The main advantage of 2D FTIR Imaging with an FPA detector relies in the spatial resolution (5.5 μm when working in reflectance mode with a 128 × 128 FPA grid), which is comparable to that of synchrotron light of 5.5 μm (i.e. each pixel has a dimension of 5.5 μm × 5.5 μm). Such spatial resolution allows to collect a large number of independent spectra on fibers, for instance more than 150 independent spectra can be typically collected on a fiber of ca. 1 mm and 10 μm thickness. By mapping the intensity of diagnostic bands in false color (red > yellow > green > blue), it is possible to see how each band is representative of the spectra of a single fiber. Besides, the detection limit of an FPA detector has been found to be significantly lower than that of a conventional mercury cadmium telluride (MCT) detector for the FTIR identification of trace amounts of materials. In fact, the heterogeneous distribution of the analyte can result in small areas of localized high concentration, which can be detected thanks to the high spatial resolution of the FTIR FPA imaging approach (Chan and Kazarian, 2006). For instance, for polyvinyl alcohol and polyvinyl acetate we verified that quantities <1 pg/pixel (1 pixel = 5.5 μm × 5.5 μm) can be detected on reflective surfaces, i.e. smaller amounts than those we typically met in the analysis of fibers.

Figs. 5–8 show representative cases. For each example reported, beside a representative spectrum of the fiber, a spectrum of the filter substrate is also shown, representative of pixels (5.5 × 5.5 μm^2 each) neighboring the fiber in the map. The bands observable in the spectra of the filter substrate include absorptions at 3625 (OH stretching of hydration water in pyllosilicates (Moenke, 1974)), 3400–3100 (OH stretching cellulose, algae (Stehfest et al., 2005)), 3000–2800 (CH stretching, algae; calcium carbonate absorptions, sediment (Ricci et al., 2006)), 2518 ($\nu_1 + \nu_3$ calcium carbonate), 1795 ($\nu_1 + \nu_4$ calcium carbonate), 1660–1640 (OH bending, water in cellulose; amide I, proteins in algae), 1560–1300 (amide II, proteins; CH_2 and CH_3 bending of organic sediment; antisymmetric CO_3^{2-} stretching, ν_3 calcium carbonate), 1200–1030 (Si-O-Si stretching, silicates; ν(C-O-C) of saccharides in algae), and 930 cm^{-1} (bending vibrations, silicates (Chen et al., 2014)).

Fig. 5 shows a dark blue fiber of ca. 30 μm thickness, that extends for more than 700 μm through the field of view of the microscope. The spectra collected on the fiber show enhanced absorption, with respect to the filter's spectra, in the 3000–2800 cm^{-1} region (CH stretching), at 1435 (δ_{as} CH_2) and 1376 cm^{-1} (δ_s CH_3), and between 3540 and 3120 cm^{-1} (OH stretching). No reproducible bands ascribable to other functional groups were observed across the fiber's surface. In this case, because no intense absorptions were observed around 1000 cm^{-1} (e.g. C—C and C—O stretching of cellulose), the assignment of the spectra to a cellulose-based fiber was uncertain. Alternatively, the CH stretching, δ_{as} CH_2, and δ_s CH_3 absorption bands could be assigned to polypropylene, while the OH stretching band (along with the OH bending centered at 1640 cm^{-1}) could be ascribed to the presence of water adsorbed on the fiber. The lower imaging contrast obtained for the bands at 1435 and 1376 cm^{-1}, as opposed to the CH stretching bands,

Fig. 6. Polypropylene - (Top left) Visible light map of the filter substrate, with marine sediments embedding a plastic microfiber. (Top right and center panels) 2D FTIR Imaging maps, where the intensity of the following bands was mapped: 2972 (ν_{as} CH_3), 1718 (ν C═O), 1469 (δ_{as} CH_2), and 1386 cm^{-1} (δ_s CH_3). The chromatic scale of each map qualitatively shows the absorbance intensity as follows: blue, green, yellow, red. Maps have dimensions of 700 × 700 μm^2 (1 tick = 50 μm). The bottom panel shows the FTIR Reflectance spectra of the plastic microfiber and of the filter substrate. Each spectrum relates to a single pixel (5.5 × 5.5 μm^2) of the 2D Imaging maps. (For interpretation of the references to color in this figure legend, the reader is referred to the web version of this article.)

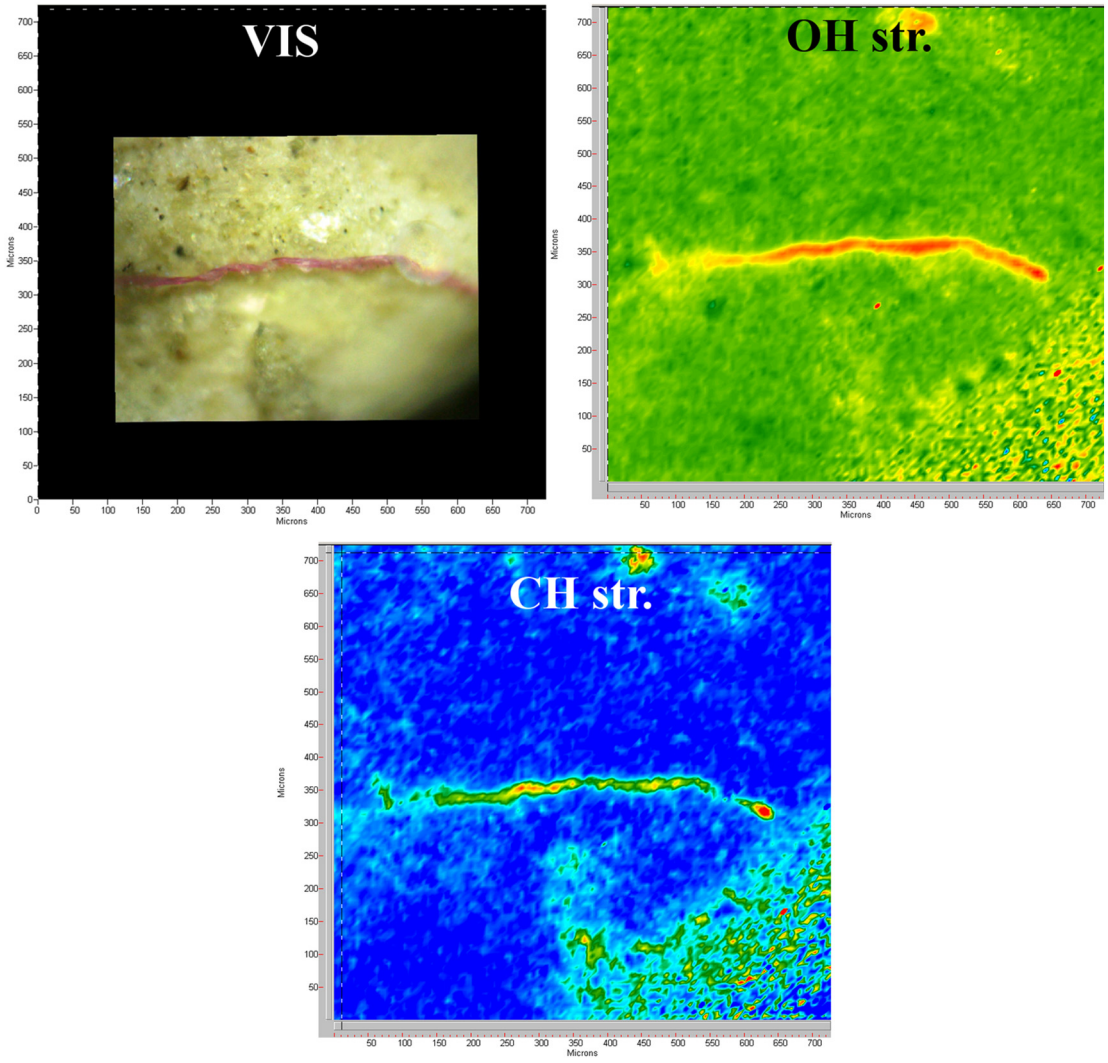
VIS
OH str.
CH str.
Microns

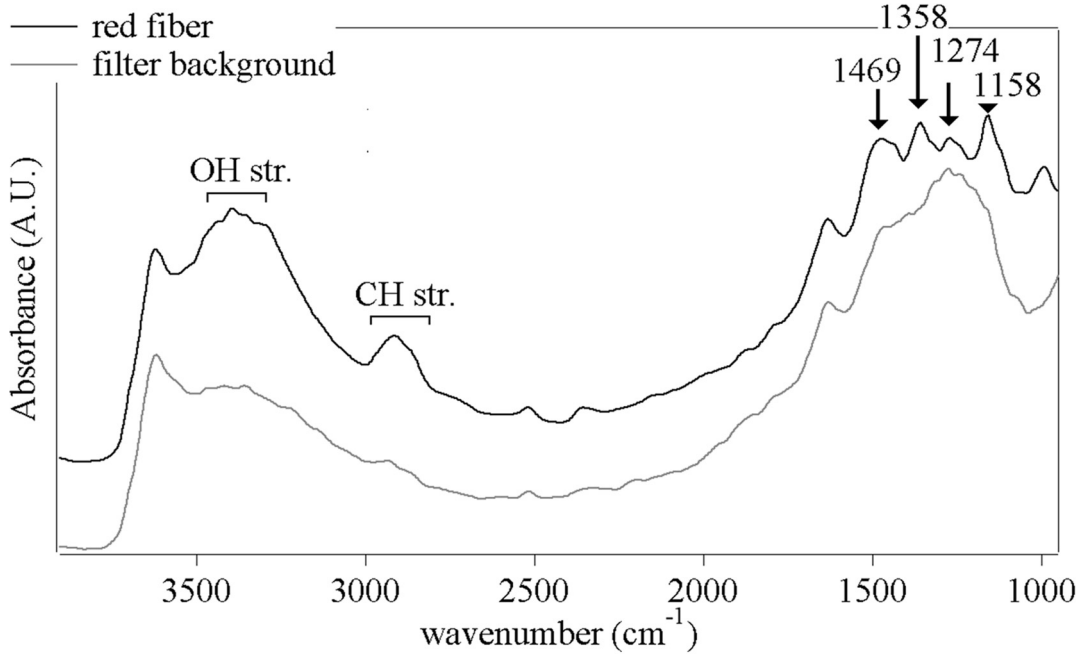
red fiber
filter background
1358
1469
1274
1158
OH str.
CH str.
Absorbance (A.U.)
3500
3000
2500
2000
1500
1000
wavenumber (cm-1)

is due to the fact that the filter substrate has intense absorptions and a high absorbance background in the fingerprint region below 1800 cm^{-1}. It must be noted that also PE has characteristic δ_{as} CH_2 and δ_s CH_3 bands around 1470 and 1370 cm^{-1}, even if the latter can be significantly weaker than that of PP, owing to the decreased number of $-CH_3$ groups (Gulmine et al., 2002).

Fig. 6 shows a dark blue fiber of ca. 50 μm thickness, almost fully embedded in the sediments on the filter substrate. Only a limited portion (ca. 200 μm long) of the fiber is visible. The spectra of the filter substrate around the fiber show intense absorptions of calcium carbonate. In particular, the presence of calcite bands at 2980, 2926 and 2854 cm^{-1} (Sanchez de Rojas e al., 2004) and the ν_3 band, showing a derivative shape (Ricci et al., 2006), made the identification of the embedded fiber particularly challenging. Nonetheless, the spectra collected on the exposed surface of the fiber show distinctive bands at 2972 (ν_{as} CH_3), 1469 (δ_{as} CH_2), and 1386 cm^{-1} (δ_s CH_3), while no bands ascribable to amides or esters were observed. The ν_{as} CH_3 band has high intensity all across the exposed fiber surface, as clearly shown in the chromatic imaging map (red pixels that match the shape of the exposed fiber surface). Instead, the δ_{as} CH_2 and δ_s CH_3 bands fall in a spectral region where the filter substrate exhibits high absorbance, corresponding to the positive peak of the intense ν_3 band of calcite. Therefore, when those bands are imaged, the exposed portion of the fiber appears as a low-absorbance area (blue pixels) in the midst of the substrate (yellow-red pixels). Finally, the fiber's spectra show an absorption band centered at 1718 cm^{-1}, clearly highlighted by the imaging map. This band was assigned to the C═O stretching of oxygenated groups, e.g. ketones and carboxylic acids (Gardette et al., 2013), which form during the abiotic oxidation of polyethylene and polypropylene (Gewert et al., 2015). Considering that oxidation rates depend strongly on used additives (either anti-oxidants as stabilizers, or pro-oxidant to favor degradation of plastics), the presence of oxidation bands can occur discontinuously in the spectra of plastic fibers belonging to the same polymer class.

Overall, 44.5% of the investigated microplastics were identified either as polypropylene or polyethylene fibers.

Fig. 7 illustrates the most problematic case that was found in this study. While enhanced absorptions between 3550 and 3100 (OH stretching region) and 3000–2800 cm^{-1} (CH stretching region) were reproducibly observed across the fiber's surface, the bands at 1469, 1358, 1274 and 1158 cm^{-1} were observed discontinuously, along with a band at 990 cm^{-1}. Because the filter substrate exhibits high absorbance in the 1800–1000 cm^{-1} region, it was not possible to obtain a neatly contrasted image of the fiber when those bands were imaged. Therefore, only a tentative assignment could be hypothesized, possible candidates being cellulose-based (owing to the strong and broad OH stretching band and to the shape of the CH stretching band) or PP fiber (which could not be completely ruled out based on the shape and position of the bands at 1469, 1358 and 1158 cm^{-1}). Even if PVC might be considered because of the bands at 1358, 1274, and 990 cm^{-1}, it must be noted that the three peaks fall at higher wavenumbers (20–25 cm^{-1} difference) than the corresponding main bands found in the transmittance spectra of PVC films, respectively 1332 (CH_2 deformation), 1255 (C—H rocking), and 959 cm^{-1} (trans C—H wagging) (Ramesh and Yi, 2008). Besides, the C—Cl stretching band of PVC falls at 610 cm^{-1}, i.e. outside the range of the FPA detector.

The identification of a polyamide fiber, which represented 32.0% of the investigated microplastics (Fig. S1) and acrylonitrile *co*-polymers (Figs. S2, S3), which represented 13.3% of the analyzed fibers, are shown in Supporting Information.

The fiber shown in Fig. 8 was identified as cellulose-based, thanks to the presence in the related spectra of a wide and intense band in the 3500–3100 cm^{-1} range (O—H stretching, hydroxyl groups of anhydroglucose unit), enhanced absorptions between 3000 and 2900 cm^{-1} (stretching of methyl and methylene C—H bonds), and a broad and intense band between 1160 and 1060 cm^{-1}, with a maximum at 1126 cm^{-1} (overlapping of C—C and C—O bands) (Canché-Escamilla et al., 2006). No reproducible diagnostic bands of functional groups ascribable to polyethylene or polypropylene, esters, PVC or polyamides were found in the spectra collected across the fiber's surface. According to the literature, rayon can be generally distinguished from natural cellulose by the absence of bands at 1735 (C═O ester stretching band from pectin), 1105 and 1050 cm^{-1} (antisymmetric and symmetric C–O–C stretching modes) (Comnea-Stanu et al., 2017), which could be the case of the fiber in Fig. 8. However, spectra of rayon fibers (bamboo rayon) with the clear presence of those bands have also been reported (Teli and Sheikh, 2013), which makes the unambiguous assignment of cellulose-based fibers to Rayon uncertain. It must be noticed that cellulose textile fibers, while not environmentally harmful per se, contain coloring agents and dyes that can be toxic to mammals and fishes. Thus, evaluating the presence of these textiles in marine sediments, along with MPs, has important environmental relevance.

4. Conclusions

The abundance and spatial distribution of MP contamination of sediments were determined across the Black Sea using samples obtained within the Joint Black Sea Survey 2017 organized within the EU/UNDP project EMBLAS-II.

A fully non-invasive method was used for analysis, which avoids bias from potential contamination of the samples and allows subsequent analysis of the filter in order to determine other classes of microplastics.

The direct identification of polymers (including PE/PP, acrylates and acrylonitrile), polyamide and cellulose-based fibers was possible in several cases. Esters were clearly identified, even though in some cases differentiating among classes with similar functional groups (e.g. acrylates, poly (vinyl acetate)) can be challenging when the filter substrate neighboring the fibers exhibits intense absorptions in the 1800–1000 cm^{-1} range. Nonetheless, the proposed methodology confirmed its potential for assessment of presence of microplastics and textile fibers in the marine environment, and in general for the non-invasive analysis of polymeric substrates. MPs were determined in 83% of samples. The average abundance in all samples was 106.7 items/kg. PE and PP, which were the most abundant polymers in this study, are also the most common plastics used in wide applications (i.e. bottle caps, food wrappers, plastic bags, packaging and fishing line). The highest pollution occurred on the North-Western shelf where the abundance of MPs was 10 times higher than in sediments from the deep sea.

According to the recent floating marine litter picture in the Black Sea Region and data observed in this study, there are no doubts that in the nearest future the abundance of marine litter in the Black Sea will grow and thus further studies on the occurrence, distribution and physical mechanisms that control how MPs reach the seafloor and govern their fate are needed in order to evaluate the environmental status of the Black Sea.

Fig. 7. Red fiber on the filter background - (Top left) Visible light map of the filter substrate, with marine sediments and a plastic microfiber lying on it. (Top right and center panels) 2D FTIR Imaging maps, where the intensity of the bands between 3550 and 3100 (OH stretching region) and 3000–2800 cm^{-1} (CH stretching region) was imaged. The chromatic scale of each map qualitatively shows the absorbance intensity as follows: blue, green, yellow, red. Maps have dimensions of 700 × 700 μm^2 (1 tick = 50 μm). The bottom panel shows the FTIR Reflectance spectra of the plastic microfiber and of the filter substrate. Each spectrum relates to a single pixel (5.5 × 5.5 μm^2) of the 2D Imaging maps. The absorptions at 1469, 1358, 1274 and 1158 cm^{-1} were observed discontinuously across the fiber surface. (For interpretation of the references to color in this figure legend, the reader is referred to the web version of this article.)

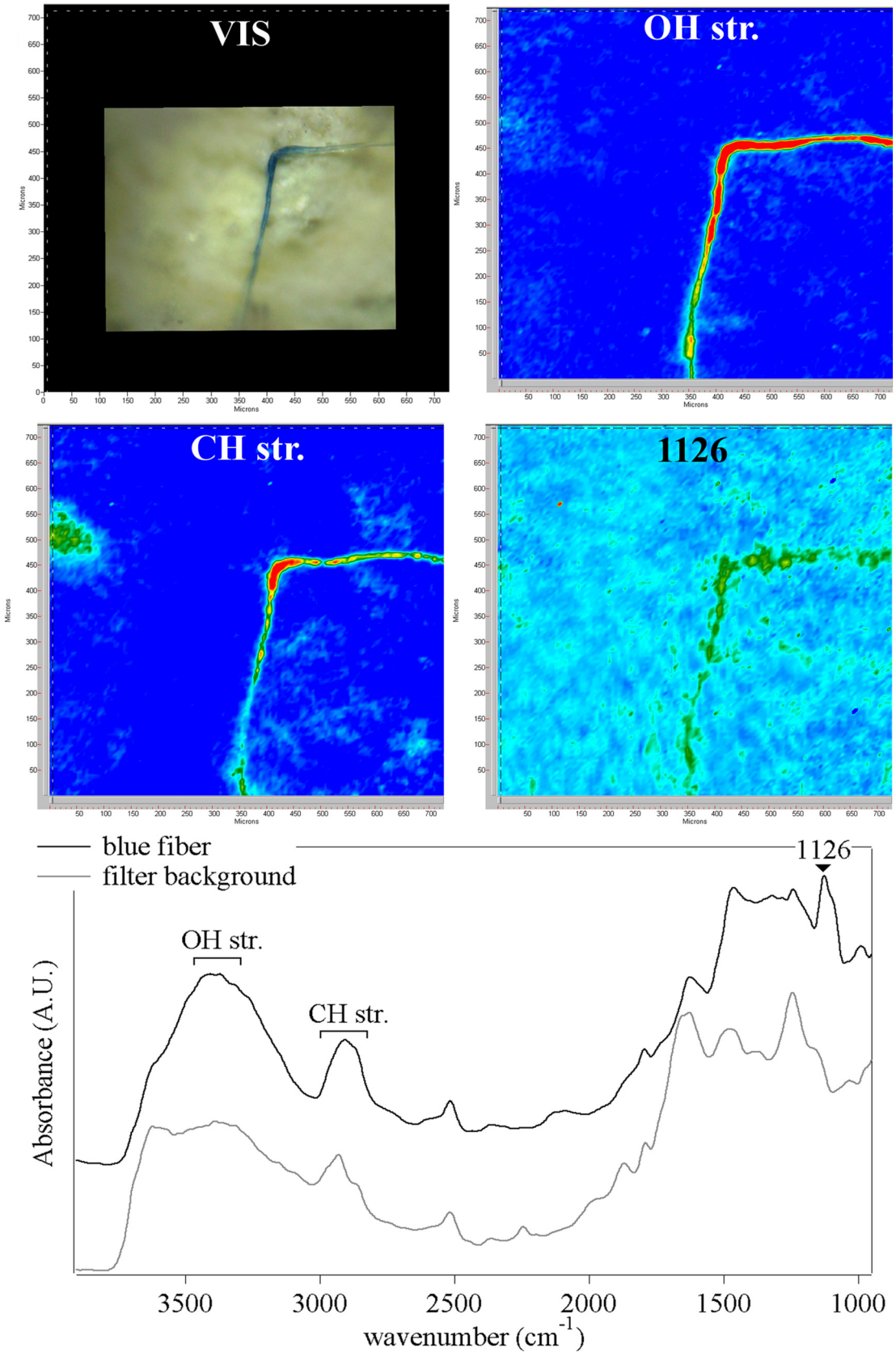

Fig. 8. Cellulose-based fiber - (Top left) Visible light map of the filter substrate, with marine sediments and a plastic fiber lying on it. (Top right and center panels) 2D FTIR Imaging maps, where the intensity of the following bands was mapped: 3500–3100 (O—H stretching), 3000–2800 (CH stretching region), and 1126 cm^{-1} (overlapping of C—C and C—O bands). The chromatic scale of each map qualitatively shows the absorbance intensity as follows: blue, green, yellow, red. Maps have dimensions of 700 × 700 μm^2 (1 tick = 50 μm). The bottom panel shows the FTIR Reflectance spectra of the plastic microfiber and of the filter substrate. Each spectrum relates to a single pixel (5.5 × 5.5 μm^2) of the 2D Imaging maps. (For interpretation of the references to color in this figure legend, the reader is referred to the web version of this article.)

Supplementary data to this article can be found online at https://doi.org/10.1016/j.scitotenv.2020.143898.

Recommendations

For more information on the extent and distribution of MPs in the Black Sea further monitoring activities with wider spatial coverage and improved sampling methodology is needed. It is recommended to enlarge the volume of sediment samples and also to make a duplicate sample from each site to receive more complete data.

CRediT authorship contribution statement

Alessandra Cincinelli – Data discussion and writing of the article

Costanza Scopetani – Measurements, MPs characterization, Revising Text

David Chelazzi – Data analysis, Data interpretation, Revising Text and Figures

Tania Martellini - Measurements, MPs characterization, Revising Text

Maria Pogojeva – Sampling, Revising text and Tables/Figures

Jaroslav Slobodnik – Data discussion, Revising text and Tables/Figures

Declaration of competing interest

The authors declare that they have no known competing financial interests or personal relationships that could have appeared to influence the work reported in this paper.

Acknowledgements

The research was supported by the EU/UNDP Project: "Improving Environmental Monitoring in the Black Sea" – Phase II (EMBLAS-II) ENPI/2013/313-169. Financial support from the Consorzio Interuniversitario per lo Sviluppo dei Sistemi a Grande Interfase (CSGI), Florence, is also gratefully acknowledged. This project has received partial funding from the European Union's Horizon 2020 research and innovation programme under grant agreement No 646063.

References

Andrades, R., Santos, R.G., Joyeux, J.-C., Chelazzi, D., Cincinelli, A., Giarrizzo, T., 2018. Marine debris in Trindade Island, a remote island of the South Atlantic. Mar. Pollut. Bull. 137, 180–184.

Andrady, A.L., 2011. Microplastics in the marine environment. Mar. Pollut. Bull. 62 (8), 1596–1605.

Aytan, U., Valente, A., Senturk, Y., Usta, R., Esensoy Sahin, F.B., Mazlum, R.E., Agirbas, E., 2016. First evaluation of neustonic microplastics in Black Sea waters. Mar. Environ. Res. 119, 22–30.

Ballent, A., Corcoran, P.L., Madden, O., Helm, P.A., Longstaffe, F.J., 2016. Sources and sinks of microplastics in Canadian Lake Ontario Nearshore, Tributary and beach sediments. Mar. Pollut. Bull. 110, 383–395.

Brien, S., 2007. Vinyls industry update. Presentation at the world vinyl forum 2007, Sept. 2007. Retrieved from. http://vinyl-institute.com/Publication/WorldVinylForumIII/VinylIndustryUpdate.aspx.

BSC, 2007. Marine Litter in the Black Sea Region: A Review of the Problem. Black Sea Commission Publications, 2007–1, Istanbul- Turkey (160 pp).

Canché-Escamilla, G., Pacheco-Catalan, D.E., Andrade-Canto, S.B., 2006. Modification of properties of rayon fibre by graft copolymerization with acrylic monomers. J. Mater. Sci. 41, 7296–7301.

Chan, K.L.A., Kazarian, S.G., 2006. Detection of trace materials with Fourier Transform Infrared Spectroscopy using a multi-channel detector. Analyst 131, 126–131.

Chelazzi, D., Chevalier, A., Pizzorusso, G., Giorgi, R., Menu, M., Baglioni, P., 2014. Characterization and degradation of poly(vinyl acetate)-based adhesives for canvas paintings. Polym. Degrad. Stab. 107, 314–320.
Devi Renuka, K.B., Madivanane, R., 2012. ESTIJ 2, 2250–3498.

Chen, Z., Hay, J.N., 2012. FTIR spectroscopic analysis of poly(ethylene terephtalate) on crystallization. Eur. Polym. J. 2012 (48), 1586–1610.

Duan, G., Zhang, C., Li, A., Yang, X., Lu, L., Wang, X., 2008. Preparation and characterization of mesoporous zirconia made by using a poly (methyl methacrylate) template. Nanoscale Res. Lett. 3, 118–122.

Chen, Y., Furmann, A., Mastalerz, M., Schimmelmann, A., 2014. Quantitative analysis of shales by KBr-FTIR and micro-FTIR. Fuel 116, 538–549.

Cincinelli, A., Scopetani, C., Chelazzi, D., Lombardini, E., Martellini, T., Katsoyiannis, A., Fosi, M.C., Corsolini, S., 2017. Microplastic in the surface waters of the Ross Sea (Antarctica): occurrence, distribution and characterization by FTIR. Chemosphere 175, 391–400.

Claessens, M., De Meester, S., Van Landuyt, L., De Clerck, K., Jaussen, C.R., 2011. Occurrence and distribution of microplastics in marine sediments along the Belgian coast. Mar. Pollut. Bull. 62 (10), 2199–2204.

Cole, M., Lindeque, P., Halsband, C., Galloway, T.S., 2011. Microplastics as contaminants in the marine environment: a review. Mar. Pollut. Bull. 62, 2588–2597.

Cole, M., Lindeque, P.K., Fileman, E., Clark, J., Lewis, C., Halsband, C., Galloway, T.S., 2016. Microplastics alter the properties and sinking rates of zooplankton faecal pellets. Environ. Sci. & Technol. 50 (6), 3239–3246.

Comnea-Stanu, I.R., Wieland, K., Ramer, G., Schwaighofer, A., Lendl, B., 2017. On the identification of Rayon/viscose as a major fraction of microplastics in the marine environment. Discrimination between material and manmade cellulosic fibers using Fourier Transform Infrared Spectroscopy. Appl. Spectrosc. 71 (5), 939–950.

Dubaish, F., Liebezert, G., 2013. Suspended microplastics and black carbon particles in the jade system, Southern North Sea. Water Air Soil Pollut., 224, art. n. 1352.

FAO, 2015. First Regional Symposium on Sustainable Small-Scale Fischeries in the Mediterranean and Black Sea, 27–30 November 2013, Saint Julian's, Malta. Edited by Abdellah Srour, Nicola Ferri, Dominique Bourdenet, Davide Fezzardi, Aurora Nastasi. FAO Fisheries and Aquaculture Proceedings, No. 39 (Rome. 519 pp).

Frias, J.P.G.L., Gago, J., Otero, V., Sobral, P., 2016. Micropalstics in coastal sediemnts from Southern Portuguese Shelf waters. Mar. Environ. Res. 114, 24–30.

Galgani, F., Hanke, G., Werner, S., et al., 2013. Guidance on Monitoring of Marine Litter in European Seas. Scientific and Technical Research SeriesPublications office of the European Union, Luxembourg.

Gardette, M., Perthue, A., Gardette, J.L., Janecska, T., Foldes, E., Pukanszky, B., Therias, S., 2013. Photo- and thermal-oxidation of polyethylene: comparison of mechanisms and influence of unsaturation content. Polym. Degrad. Stab. 98, 2383–2390.

Gewert, B., Plassmann, M.M., MacLeod, M., 2015. Pathways for degradation of plastic polymers floating in the marine environment. Environ. Sci.: Processes Impacts 17, 1513–1521.

Goldberg, E.D., 1997. Plasticizing the seafloor: an overview. Environ. Technol. 18, 195–201.

Grover, N., Singh, H., Gupta, B., 2010. Characterization of acrylic acid grafted poly(ethylene terephtalate) fabric. J. Appl. Polym. Sci. 117, 3498–3505.

Gulmine, J., Janissek, P.R., Heise, H.M., Akcelrud, L., 2002. Polyethylene characterization by FTIR. Polym. Test. 21 (5), 557–563.

Harrison, J.P., Ojeda, J.J., Romero-Gonzalez, M.E., 2012. The applicability of reflectance micro-Fourier-transform infrared spectroscopy for the detection of synthetic microplastics in marine sediments. Sci. Total Environ. 416, 455–463.

Kane, I.A., Clare, M.A., 2019. Dispersion accumulation and the ultimate fate of microplastics in deep marine environments: a review and future directions. Fron. Earth Sci., vol. 7, art. 80.

Lechner, A., Keckeis, H., Lumesberger-Loisl, F., Zens, B., Krush, R., Tritthart, M., Glas, M., Schludermann, E., 2014. The Danube so colorful: a potpourri of plastic litter outnumbers fish larvae in Europe's second largest river. Environ. Pollut. 188, 177–181.

Lobelle, D., Cunliffe, M., 2011. Early microbial biofilm formation on marine plastic debris. Mar. Pollut. Bull. 62, 197–200.

Löder, M.G.J., Kuczera, M., Mintenig, S., Lorenz, C., Gerdts, G., 2015. Focal plane array detector-based micro-Fourier-transform infrared imaging for the analysis of microplastics in environmental samples. Environ. Chem. 12, 563–581.

Lusher, A.L., McHugh, M., Thompson, R.C., 2013. Occurrence of microplastics in the gastrointestinal tract of pelagic and demersal fish from the English Channel. Mar. Pollut. Bull. 67, 94–99.

Lusher, A., 2015. Microplastics in the marine environment: distribution, interactions and effects. In: Bergmann, M., Gutow, L., Klages, M. (Eds.), Mar. Anthropogenic Litter. Springer, Berlin, pp. 245–308.

Matsugama, Y., Takada, H., Kumata, H., Kauke, H., Sakurai, S., Suzuki, T., Itoh, M., Okazaki, Y., Boonyattumamond, R., Zakaria, M.P., Weerts, S., Newman, B., 2017. Microplastics in sediments cores from Asia and Africa as indicators of temporal trends in plastic pollution. Arch. Environ. Contam. Toxicol. 73, 230–239.

Moenke, H.H.W., 1974. Silica, the three-dimensional silicates, borosilicates, and beryllium silicates. In: Farmer, V.C. (Ed.), Infrared Spectra of Minerals. Mineralogical Society, London, pp. 365–382.

Obbard, R.W., Sadri, S., Wang, Y.-Q., Khitun, A., Baker, I., Thompson, R.C., 2014. Global warning releases microplastic legacy frozen in Arctic sea ice. Earth's Future https://doi.org/10.1002/2014EF000240.

Peng, G., Zhu, B., Yang, D., Su, L., Shi, H., Li, D., 2017. Microplastics in sediments of the Changjiang Estuary, China. Environ. Poll. 225, 283–290.

Porubuska, M., Szollos, O., Konov, A., Janigova, Jaskova, M., Jomova, K., Chodak, O., 2012. FITR spectroscopy study of polyamide-6 irradiated by electron and proton beams. Polym. Degrad. Stab. 97, 523–531.
Pockett, P., 2004. Crystallinity in Linear Polyamides: a Study Using Melt Blending with Small-molecule Diluents. Thesis. University of South Australia 2004. Appendix C pp. 335–337.

Quinn, B., Murphy, F., Ewins, C., 2017. Validation of density separation for the rapid recovery of microplastics from sediment. Anal. Meth. 9, 1491–1498.

Ramesh, S., Yi, L.J., 2008. FTIR spectra of plasticized high molecular weight OVC-$LiCF_3SO_3$ electrolytes. Ionics 15, 413–420.

Ricci, C., Miliani, C., Brunetti, B.G., Sgamellotti, A., 2006. Non-invasive identification of surface materials on marble artifacts with fiber optic mid-FTIR reflectance spectroscopy. Talanta 1221–1226.

Sanchez de Rojas, M.I., Azorin, V., Frias, M., Rivera, J., Garcia, N., Martin-Estarlich, A., 2004. Weathering, cleaning and conservation of the brick façade on the "Niño Jesus" Hospital in Madrid. In: Saiz-Jimenez (Ed.), Air Pollution and Cultural Heritage. Taylor & Francis Group, London.

Scopetani, C., Chelazzi, D., Cincinelli, A., Esterhuizen-Londt, M., 2019. 2019. Assessment of microplastic pollution: occurrence and characterisation in Vesijärvi lake and Pikku Vesijärvi pond, Finland. Environ. Monit. Assess. 191 (11), 652.

Scopetani, C, Esterhuizen-Londt, M, Chelazzi, D, Cincinelli, A, Setälä, H, Pflugmacher, S, 2020. Self-contamination from clothing in microplastics research. Ecotoxicol Environ Saf 189 (110036).

Slobodnik, J., Alexandrov, B., Komorin, V., Mikaelyan, A., Guchmanidze, A., Arabidze, M., Korshenko, A., Moncheva, S., December 2017. National Pilot Monitoring Studies and Joint Open Sea Surveys in Georgia, Russian Federation and Ukraine, 2016 Final Scientific Report, EU/UNDP Regional Bureau for Europe and the CIS Project: Improving Environmental Monitoring in the Black Sea – Phase II (EMBLAS-II), ENPI/2013/313-169.

State of the Black Sea Environmental, 2002. National Report of Ukraine 1996–2000. Ministry of Ecology and Natural Resources of Ukraine. Astoprint, Odessa.

Stehfest, K., Toepel, J., Wilhelm, C., 2005. The application of micro-FTIR spectroscopy to analyze nutrient stress-related changes in biomass composition of phytoplankton algae. Plant Physiol. Biochem. 43, 717–726.

Tagg, A.S., Sapp, M., Harrison, J.P., Ojeda, J.J., 2015. Identification and quantification of microplastics in wastewater using focal plane array-based reflectance micro-FT-IR imaging. Anal. Chem. 87, 6032–6040.

Teli, M.D., Sheikh, J., 2013. Study of grafted silver nanoparticle containing durable antibacterial bamboo rayon. Cell. Chem.Technol. 47 (1), 69–75.

Vianello, A., Boldrin, A., Guerriero, P., Moschino, V., Rella, R., Sturaro, A., Da Ros, L., 2013. Microplastic particles in sediments of Lagoon of Venice, Italy: first observations on occurrence, spatial patterns and identification. Estuar. Coast. Shelf Sci. 130, 54–61.

Woodall, L.C., Sanchez-Vidal, A., Canals, M., Paterson, G.L.J., Coppock, R., Sleight, V., Calafat, A., Rogers, A.D., Narayanaswamy, B.E., Thompson, R.C., 2014. The deep sea is a major sink for microplastic debris. R. Soc. Open Sci. 1, 140317.